RETURN TO ISSUE | < PREV | ARTICLE | NEXT >

Embellishing 2-D MoS_2 Nanosheets on Lotus Thread Devices for Enhanced Hydrophobicity and Antimicrobial Activity

Govarthini Seerangan Selvam, Thangaraju Dheivasigamani*, Anusha Prabhu, and Naresh Kumar Mani*

Cite this: *ACS Omega* 2022, 7, 28, 24606–24613
Publication Date: July 6, 2022
https://doi.org/10.1021/acsomega.2c02337

SUBJECTS: Absorption, Cellulose, Fibers, Hydrophobicity, Two dimensional materials

Abstract

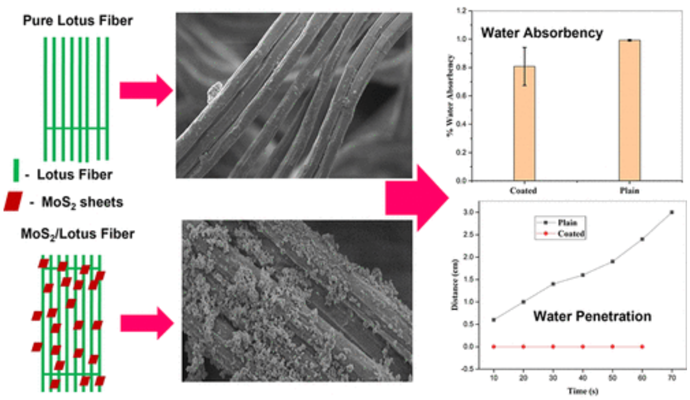

Herein, we report cellulose-based threads from Indian sacred Lotus (*Nelumbo nucifera*) of the Nymphaceae family embellished with MoS_2 nanosheets for its enhanced hydrophobic and antimicrobial properties. MoS_2 nanosheets

ACS Publications
Most Trusted. Most Cited. Most Read.

X-ray diffractometry (XRD) and scanning electron microscopy (SEM). The XRD pattern of pure lotus threads showed a semicrystalline nature, and the threads@MoS_2 composite showed more crystallinity than the pure threads. SEM depicts that pure lotus threads possess a smooth surface, and the MoS_2 nanosheets growth can be easily identified on the threads@MoS_2. Further, the presence of MoS_2 nanosheets on threads was confirmed with EDX elemental analysis. Antimicrobial studies with *Escherichia coli* and *Candida albicans* reveal that threads@MoS_2 have better resistance than its counterpart, i.e., pure threads. MoS_2 sheets play a predominant role in restricting the wicking capability of the pure threads due to their enhanced hydrophobic property. The water absorbency assay denotes the absorption rate of threads@MoS_2 to 80%, and threads@MoS_2 shows no penetration for the observed 60 min, thus confirming its wicking restriction. The contact angle for threads@MoS_2 is 128°, indicating its improved hydrophobicity.

1. Introduction

Jump To

Lotus, an aquatic perennial widely cultivated in India, Asia, Australia, China, and Japan, typically grows in swamps and shallow waters. (1) The natural cellulose from lotus fibers is associated with continuous rings inside the peduncles lying under the epidermis of vascular tissue. (2−5) The lotus leaf's excellent and stable superhydrophobicity is due to a combination of optimal traits such as surface topography, toughness, and the epicuticular wax's unique qualities. The Lotus effect has encouraged researchers to create superhydrophobic surfaces and to design materials with enhanced hydrophobicity obtained from the lotus fibers. (6)

Nanomaterials have played a prominent role in altering size and structure at the nanoscale level to achieve and mimic the property mentioned above. 2D materials are currently recognized as nanomaterials having a sheetlike shape and a substantial lateral dimension ranging from hundreds of nanometers to tens of micrometers or even greater but only a single or few atomic layer thickness. Transition-metal dichalcogenides, noble metal dichalcogenides, MXenes, hexanol boron nitride, organics/polymers, and transition-metal halides are some examples of innovative 2D materials beyond graphene. (7) Of these, transition-metal dichalcogenides (TMDCs) have a one-of-a-kind amalgamation in-direct bandgap, approving electronic and mechanical properties, spin−orbit solid coupling, and thickness on the atomic scale, making them appealing for elementary research as well as applications that include personalized medicine, flexible electronics, high-end electronics, energy harvesting, DNA sequencing, optoelectronics, and spintronics. (8,9) TMDCs are made up of three atomic planes and often two atomic species: a metal and two chalcogens. TMDCs have a generic formula of MX_2 where M denotes transition metal and (M = V, Zr, Ti, Ta, Hf, Nb, W, Co, Tc, Ir, Re, Pd, Rh, Ni, Mo, and Pt) and X denotes chalcogen (X= Te, S, and Se). The layered metal chalcogenides encompass a wide range of electrical characteristics from real metals (NbS_2) to superconductors (TaS_2) to semiconductors (MoS_2) with a wide variety of bandgaps and offsets. (9,10)

Abstract

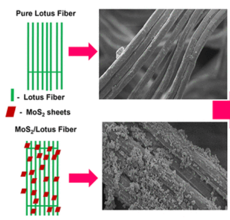

Figure 1

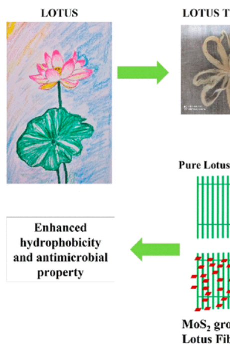

Figure 1. Schematic ill
coating 2D-MoS_2 nanc
lotus threads.

Figure 2

(11−13) Since then, several nanoscience and nanotechnology journals have focused on the area of 2D materials. MoS_2 possesses a hexagonal arrangement consisting of S−Mo−S covalent bonds, and between the neighboring layers of MoS_2 there is a van der Waals interaction that allows them to be mechanically separated to form two-dimensional nanosheets. (14) The two-dimensional MoS_2 nanosheets have various physical and chemical properties and possess several applications. Recent research on MoS_2 has revealed this as a solitary contender in hydrogen storage, supercapacitors, sensors, electrocatalysis, and other applications such as electronic sensors, biomedical engineering, and other applications. The remarkable unique properties include a great amount of surface area and absorption in the near-infrared band, thus providing a new outcome in biological applications. (15) Biomedical uses for 2D MoS_2 sheets have been recently explored as well. In their seminal work, Zhu et al. explained that MoS_2 monolayers could be used to identify DNA molecules based on their fluorescence quenching capabilities. MoS_2 sheets have been employed as an NIR photothermal agent to kill Hela cells using their near-infrared (NIR) absorption. It has been reported that PEG-functionalized MoS_2 sheets can be used to transport drugs. (16)

The utilization and manipulation of the thread's wicking qualities for building programmable microfluidic channels have been the focus of thread-based research. So far, researchers have been looking for appealing substrate materials for decades to keep microfluidics advancing and overcome the disadvantages and difficulties such as tedious and expensive fabrication methods. Because of their unique structural and mechanical qualities, cellulose substrates such as thread and paper are considered as viable solutions for various applications. (17−21) Thread has demonstrated many potential applications in diagnostic systems, smart bandages, and tissue engineering. (22) Thread-based microfluidics is still in its infancy, and additional developments in manufacturing, analytical methodologies, and function are required before they can be commercialized as low-cost, low-volume, and simple-to-use point-of-care (POC) diagnostic devices. (23−26) Because of its features like flexibility, portability, biodegradability, lightweight, high tensile strength, and availability, several attempts have been made to employ thread for low-cost diagnostics or detection, among other low-cost materials such as paper and plastic. (27−30) Liquid wicking in the thread is caused by the twisted strands of cellulose fiber and the space between them.

In this work, for the first time, we have incorporated 2D TMDC MoS_2 nanomaterials on natural threads obtained from lotus fibers (Figure 1). Since MoS_2 nanocomposites are widely used for diode fabrication, (31) dye removal processes, (32) high-performance microwave absorbers, (33) fuel oil separation, (34) tunable microwave absorbers, (35) and electromagnetic wave absorption capability, (36) the idea of drop-casting 2D-nanomaterials on a cellulose fiber can offer a different perspective for wearable sensors. Integration of thread devices (natural and synthetic) with 2D nanomaterials for enhanced hydrophobicity and antimicrobial activity remains unexplored. There has been an increasing interest in discovering and producing novel antimicrobial agents from numerous sources in recent years to tackle microbial resistance. As a result, antimicrobial activity screening and evaluation methodologies have received more attention. (37) Antimicrobial susceptibility

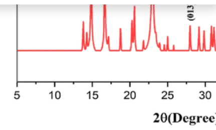

Figure 2. Comparative
of lotus fiber and calc
Iβ cellulose patterns.

Figure 3

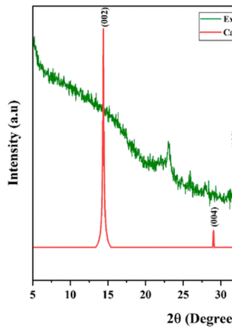

Figure 3. Comparative
of MoS_2@fiber and ca
MoS_2.

Figure 4

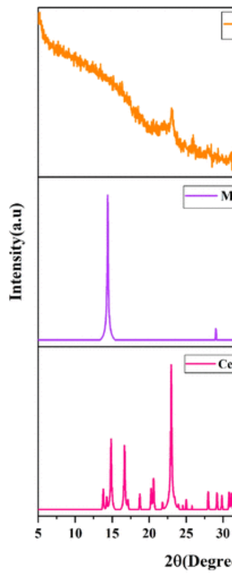

Figure 4. Comparative
fiber@MoS_2 with CIF
4114994 and 900766
and MoS_2, respectivel

Figure 5

threads@MoS_2 are assessed for their potential antimicrobial properties against *Escherichia coli* and *Candida albicans* under light and dark conditions. MoS_2 was synthesized using the coprecipitation technique and further characterized through XRD and FESEM. (39)

Figure 1

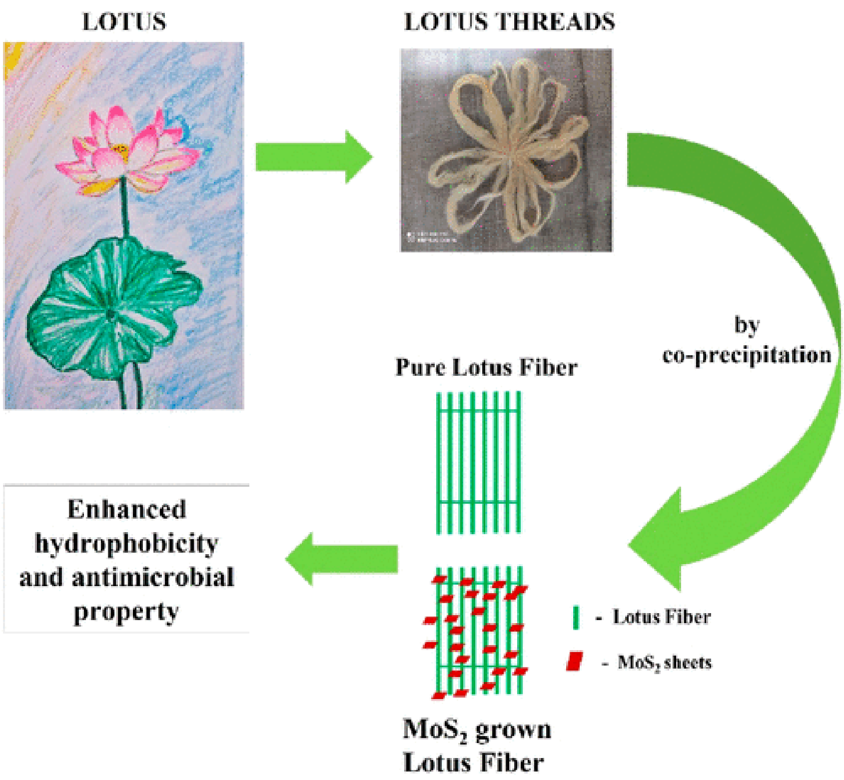

Figure 1. Schematic illustration of coating 2D-MoS_2 nanosheets on lotus threads.

2. Experimental Methods

Jump To

2.1. Materials Used

Chemicals used in this research work were used as purchased. Sodium molybdate dihydrate ($Na_2MoO_4{\cdot}2H_2O$, Sisco laboratories, 99%), thioacetamide (CH_3CSNH_2, Loba Chemie, 99%), and hydrochloric acid (HCl, Merck Life, 37%) were purchased. Standard strains of *E. coli* (ATCC 25922) and *C. albicans* (ATCC 24433) were obtained for testing antimicrobial properties from the Department of Microbiology, Kasturba Medical College, Manipal. Nutrient Agar and Sabouraud Dextrose Agar with chloramphenicol were procured from Himedia, India.

2.2. Extraction of Lotus Fiber

Lotus stems were collected at Kolarampathy Lake in Coimbatore, Tamil Nadu, with a latitude of ~10.973400° and longitude of ~76.909850°. Ideally, flowers should be fully bloomed so that the deep pink blooms contain the finest lotus fibers. The collected fibers are then trimmed, snapped, and twisted. The twisted fibers reveal 20–30 fine white filaments pulled and wrapped into a single thread.

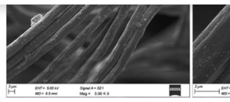
Figure 5. Different ma
SEM images (a–d) of
fiber.

Figure 6
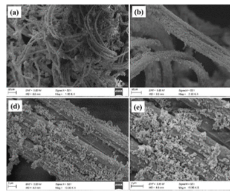
Figure 6. Different ma
SEM images (a–e) an
MoS_2-coated lotus fib

Figure 7
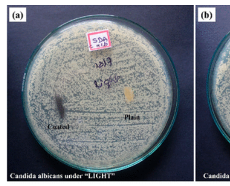
Figure 7. Antifungal a
and MoS_2-coated lotu
light (a) and dark (b) c

Figure 8
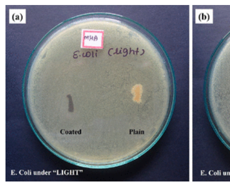
Figure 8. Antibacterial
pure and MoS_2-coate
under light (a) and da
conditions.

Figure 9
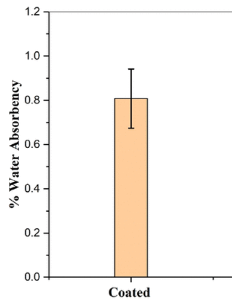

mmol of CH_3CSNH_2 was added to the above solution. The well-washed (with Millipore water and ethanol) lotus fiber thread was dipped inside the solution, and then the solution was heated to 65 °C. HCl was included dropwise to the mother solution at 65 °C. The colorless solution turned dark blue. The heat treatment continued, and a color change from dark blue to brown and then eventually to chocolate brown within 10 min of adding HCl was observed. The temperature of the solution was maintained at 80 °C for 1 h. The particles were left overnight for the settlement. The collected particles, which were then centrifuged for 10 min at 3500 rpm, were washed and dried at 55 °C and collected.

2.4. Characterization

The structure of the coated fiber was examined by a Philips PAN analytical Xpert pro powder X-ray diffractometer with Cu Kα (1.54 Å). Morphology and elemental analysis of pure and MoS_2-coated lotus fiber were recorded using an S-3400 N Hitachi field emission scanning electron microscope (FESEM).

The hydrophobicity of the uncoated and MoS_2 nanoparticle-coated lotus fiber threads (3 cm length) was assessed by measuring the water penetration rate in the thread pieces. A 100 μL portion of phenol red dye solution in water was added to one end of the threads placed over an overhead projector (OHP) sheet, and images of the threads were captured at defined time intervals using a Canon Eos 3000D DSLR camera and further analyzed using FIJI software.

The water absorbency of the uncoated and coated fibers (1 cm length) was determined by measuring the dry weight of the threads using a weighing balance then dipping the thread pieces in 1 mL of water for 5 min to measure the wet weight of the threads. The percentage of water absorbency was measured using the following formula:

$$\%\ \text{water absorbency} = \frac{\text{wet weight} - \text{dry weight}}{\text{wet weight}} \times 100 \quad (1)$$

The contact angle measurements for the uncoated and coated fibers were analyzed using the KYOWA Interface Measurement and Analysis System through a sessile drop method.

2.5. Antimicrobial Properties

Culture suspensions of *E. coli* and *C. albicans* spiked in water were prepared, adjusted to 0.5 McFarland standard concentration, and inoculated on Muller Hinton Agar (MHA) and Sabouraud Dextrose Agar (SDA) with chloramphenicol, respectively. The uncoated and MoS_2 nanoparticle-coated lotus fiber threads (UV sterilized, 10 mm length) were placed on the agar media in the inoculated plates and incubated under two different conditions to check the antimicrobial property of the threads. The first plate was incubated at 37 °C under ambient

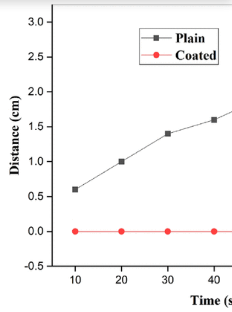

Figure 10. Water pene
of pure and MoS_2-coa

Figure 11

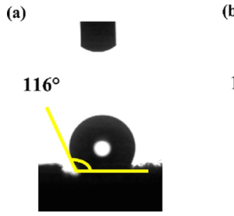

Figure 11. Contact ang
and MoS_2-coated fibe

3.1. Structural Studies

XRD analysis of Pure and MoS_2 coated lotus thread was carried out for analyzing its structure. Patterns of pure lotus fibers were well matched with cellulose crystalline standards. Observed XRD reflections of lotus fibers are well-matched with the cotton Iβ cellulose. The cotton Iβ cellulose reference pattern was taken from CIF file no. 4114994 using the Mercury 3.8 program. (40) Comparative patterns of experimental (fiber) and calculated (cotton Iβ cellulose) are depicted in Figure 2. The comparison clearly shows that the obtained major reflection for lotus fiber planes such as (1−10), (110), (102), and (200) were well matched with the calculated one with a broader pattern. The recorded pattern of fiber@MoS_2 is presented in Figure 3 and was compared with the calculated standard with CIF file no. 9007660 of MoS_2, (41) which exhibits a hexagonal structure. The obtained composite pattern clearly shows that the broad pattern at (002) reveals the thin layers of MoS_2 sheets. Mugashini et al. confirm the thin layer of MoS_2 nanosheets. (42,43) The high crystalline peak of MoS_2 at the (100) plane supports the island growth nature of MoS_2.

Figure 2

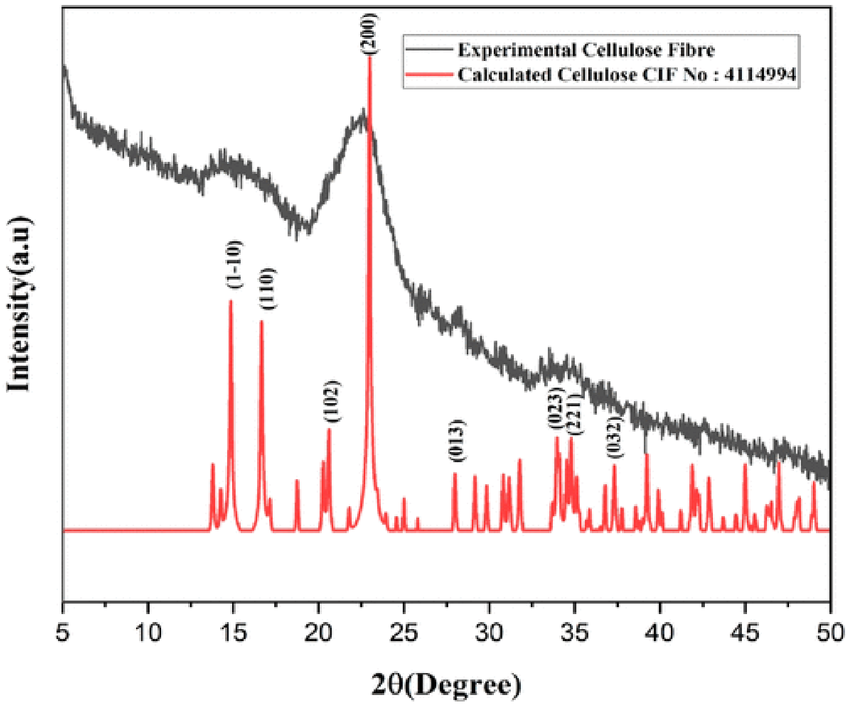

Figure 2. Comparative XRD pattern of lotus fiber and calculated cotton Iβ cellulose patterns.

Figure 3

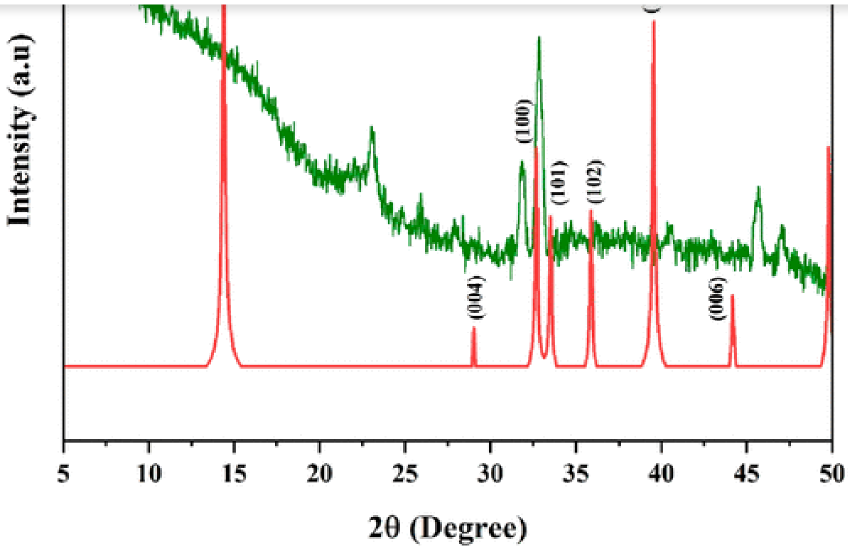

Figure 3. Comparative XRD pattern of MoS_2@fiber and calculated MoS_2.

The sharp intensity patterns on cellulose and fiber@MoS_2 at 2θ = 14.3° and 23°, corresponding to (002) and (200) planes, respectively, are examined. Figure 4 confirms the improved crystalline nature of lotus fibers after acid treatment. The sharp reflection at the (200) plane supports the fiber@MoS_2 containing the crystalline cellulose. (44) Generally, MoS_2 has a sheetlike structure spread on the surface in addition to the island (pitted) growth. The (002) plane appears broader (thin layers of MoS_2), which is due to the sheet structures, and the planes (100), (101), (102), and (103) confirm the island formation.

Figure 4

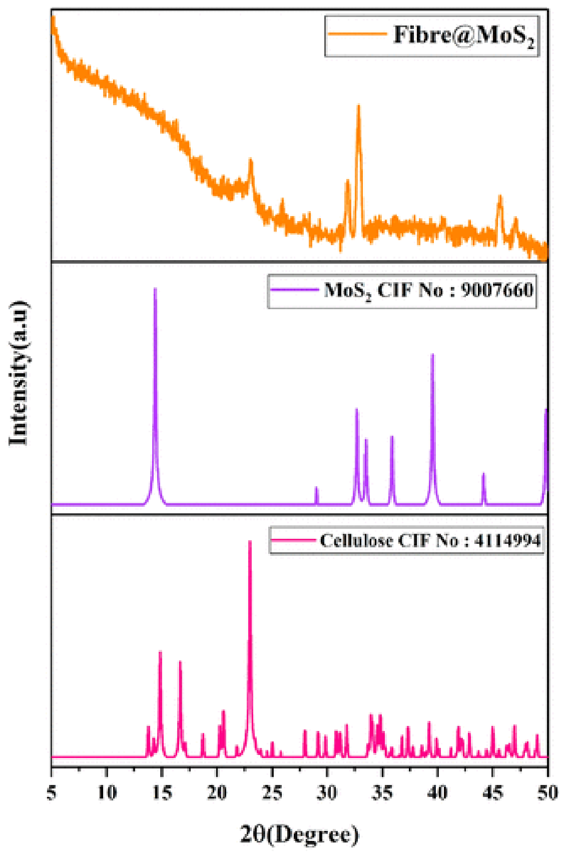

Figure 4. Comparative XRD data of fiber@MoS_2 with CIF File Nos. 4114994 and 9007660 of cellulose and MoS_2, respectively.

and EDX of MoS_2-coated fibers. Excellent moisture absorption and permeability due to the twisted ribbon-like structure were observed. The twisted helical structures of the fibers are observed. With increasing magnification, the H-shaped cuts required for water transportation are visible. Fibers appear slender, and veins are seen in the transverse view of the fiber. The cracks that occurred during fiber extraction are noticed. Damaged areas with cracks result in a fine layer of MoS_2 nanosheets. The nanosheets arise vertically on the fiber's surface, which also appears as H-cuts. The appearance of frequent H-cuts makes fiber water repellent. The diameter of the pure fiber is 2.92 μm, whereas the diameter of fiber@MoS_2 is 2.89 μm.

Figure 5

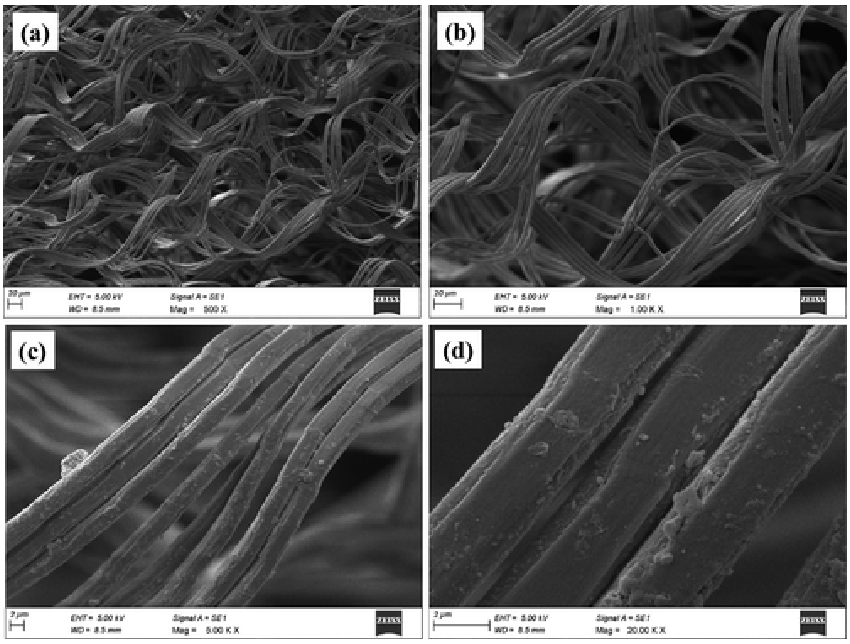

Figure 5. Different magnification SEM images (a–d) of pure lotus fiber.

Figure 6

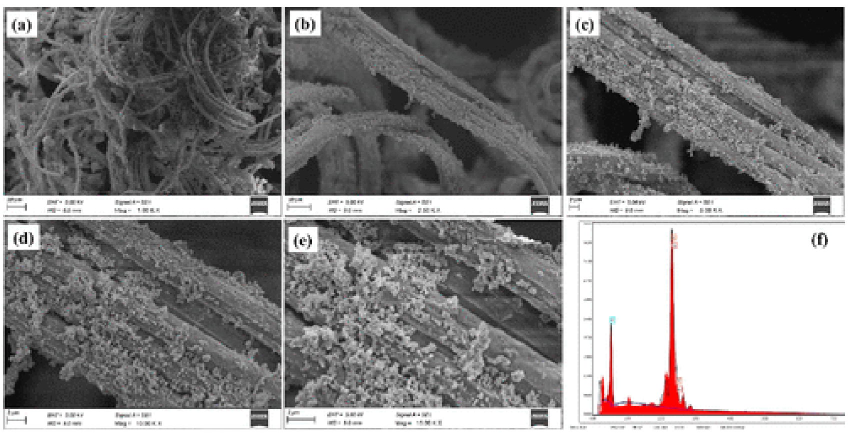

Figure 6. Different magnification SEM images (a–e) and EDX (f) of MoS_2-coated lotus fiber.

3.3. Antifungal Activity

organism cultures, and the zone of inhibition of growth around the discs is studied to determine the antimicrobial property of the test compound. (37,45−47) Similarly, in our study, we have checked for the presence of a zone of inhibition of growth formed around the uncoated and MoS_2 nanosheet coated lotus fiber threads placed on the agar media plates inoculated with *C. albicans* culture and were further incubated at 37 °C. Under ambient light conditions, the MoS_2-coated thread exhibited more antifungal activity than the uncoated or plain thread (Figure 7a). Similarly, the MoS_2-coated thread exhibited more antifungal activity under dark conditions than the uncoated or plain thread (Figure 7b).

Figure 7

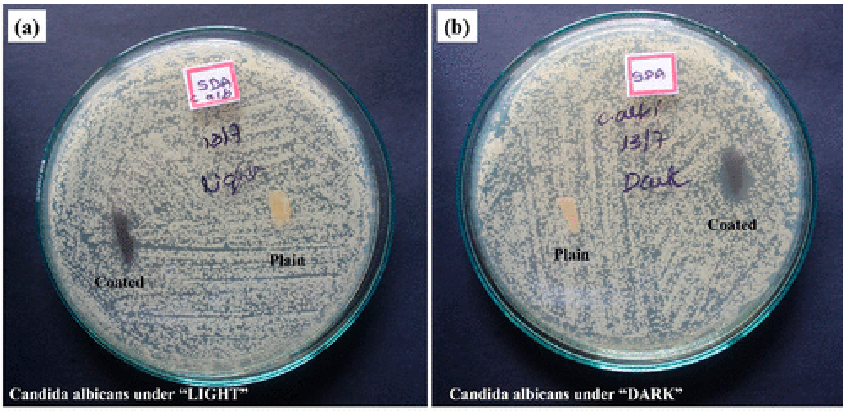

Figure 7. Antifungal activity of pure and MoS_2-coated lotus fiber under light (a) and dark (b) conditions.

Interestingly, the zone of inhibition (ZOI) in the dark was more prominent than in the light experiments. We hypothesize that this may be due to the photosensitive nature of MoS_2 nanosheets in the presence of ambient light and dark conditions. The study confirms that the growth of fungi *C. albicans* around the uncoated or plain lotus threads is attributed to no antifungal activity.

3.4. Antibacterial Activity

Figure 8 represents the antibacterial activity of uncoated and MoS_2-coated lotus threads under ambient light and dark conditions. Antibacterial activity of the MoS_2-coated lotus fiber thread was observed mainly under the dark conditions, depicted by the zone of inhibition of growth of *E. coli* formed around the coated thread. However, significant growth of the organism was observed around the uncoated or plain thread under both ambient light and dark conditions exhibiting no antibacterial activity. Thus, the antimicrobial studies conducted confirm the more antibacterial and antifungal activity of the coated nanoparticle lotus fiber threads under dark conditions than in ambient light. MoS_2 nanosheets can generate ROS and induce physical damage for bacterial inactivation. (48) Similarly, Basu et al. have shown the antifungal and antipollutant activity of MoS_2 nanosheets under dark conditions. (49) In their seminal work, Alimohammadi et al. reported that peptidoglycan mesh in the bacterial cell wall has been indicated as a primary target for interaction with the sheets leading to morphological changes and cell wall damage. (50) A comparative table depicting the antimicrobial activity of MoS_2 by various

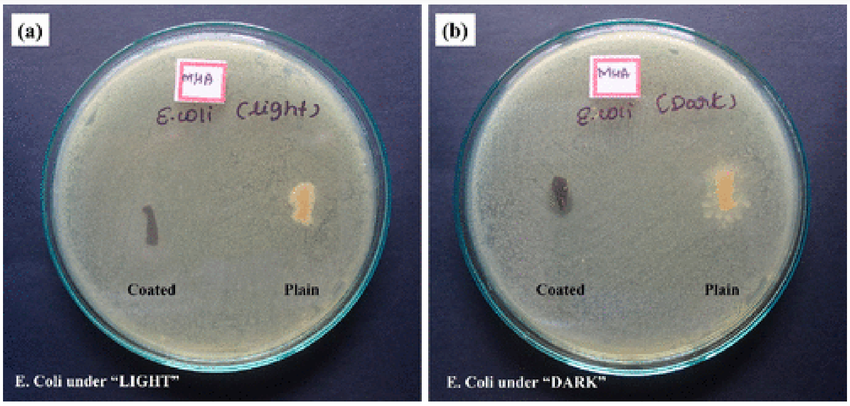

Figure 8. Antibacterial activity of pure and MoS_2-coated lotus fiber under light (a) and dark (b) conditions.

3.5. Water Absorbance and Penetration Assay

On plain lotus fiber, the water absorbance is relatively high. Liu et al. confirmed the rate of faster absorption of water in the lotus fiber. (53) On the other hand, lotus fiber coated with nanostructured MoS_2 has low absorbance, making it water resistant, which can be potentially integrated with fabrics. Figure 9 shows the water absorbency graph on pure and MoS_2-coated fiber, which indicates that coated fibers tend to absorb about 80% when compared with the absorption of uncoated fibers. Figure 10 gives the graphical representation for lateral water penetration on plain and MoS_2-coated fibers. Water penetration on plain lotus fiber increases gradually over a distance of 3 cm for the observed 60 min, whereas the fiber@MoS_2 shows no penetration, i.e., 0 cm for 60 min. Thus, the water penetration assay confirmed that no penetration occurs in fiber@MoS_2.

Figure 9

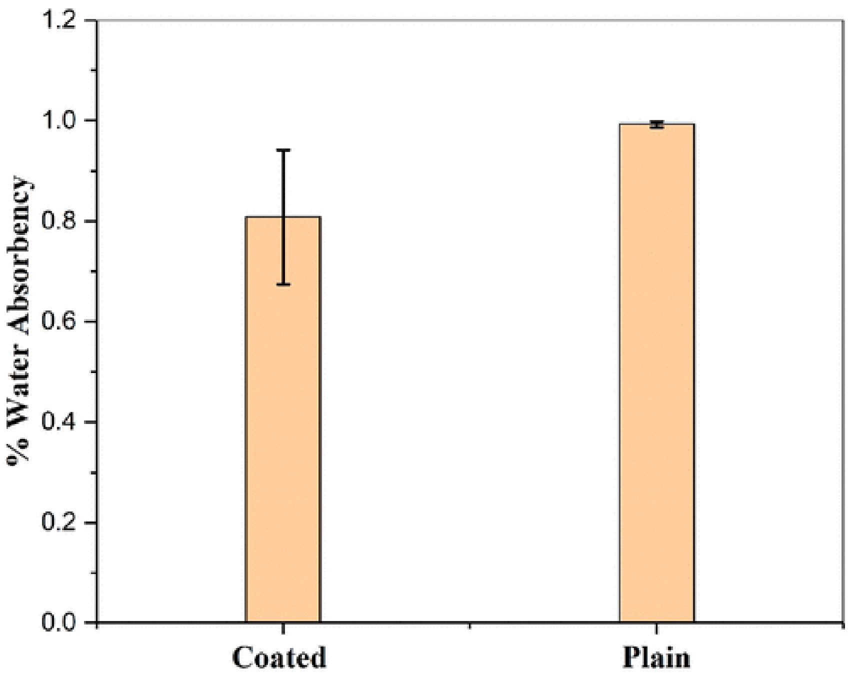

Figure 9. Water absorbency of pure and MoS_2-coated lotus fiber.

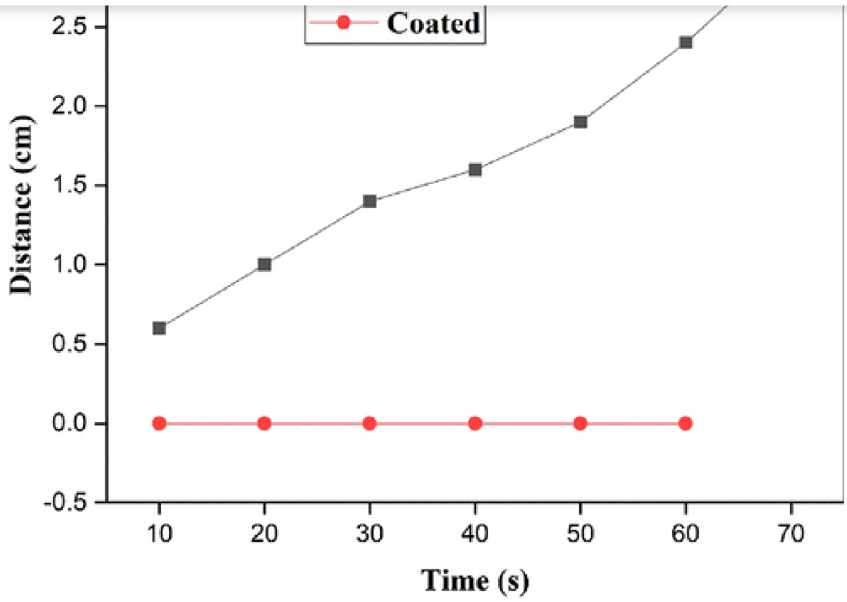

Figure 10. Water penetration assay of pure and MoS_2-coated lotus fiber.

3.6. Contact Angle Measurements

Figure 11 shows the contact angle measurements of pure (a) and MoS_2-coated lotus fiber (b). Observation inferred that pure fiber makes a contact angle of 116°, and MoS_2-coated lotus fiber has a contact angle of 128°, indicating that MoS_2 coating improves the hydrophobicity of fiber. The contact angle value increases toward superhydrophobicity.

Figure 11

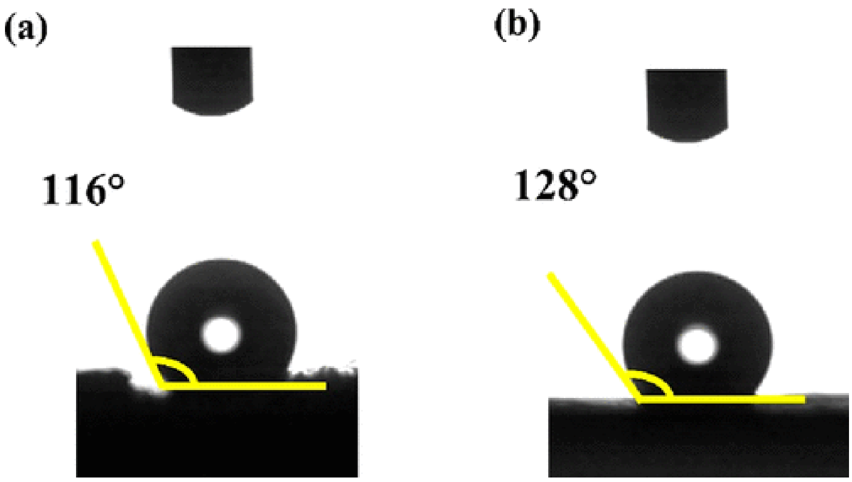

Figure 11. Contact angle of pure (a) and MoS_2-coated fiber (b).

4. Conclusion

Jump To

The coprecipitation method was used to assess the hydrophobicity and antimicrobial activity of MoS_2 nanosheets coated on lotus fiber. The XRD patterns confirmed the crystalline nature of pure fiber and fiber@MoS_2. FESEM reveals the morphology of fiber@MoS_2. The growth of MoS_2 nanoparticles over the fiber decreases the wicking ability, confirming the hydrophobic nature of the material. Further, antibacterial and antifungal activities of the MoS_2-coated fiber were verified with *E. coli* and *C. albicans*, respectively. The contact angle of

Supporting Information

Jump To

The Supporting Information is available free of charge at https://pubs.acs.org/doi/10.1021/acsomega.2c02337.

- Antimicrobial activity of MoS_2 nanosheets (Table S1) (PDF)

Embellishing 2-D MoS_2 Nanosheets on Lotus Thread Devices for Enhanced Hydrophobicity and Antimicrobial Activity

Embellishing 2-D MoS_2 Nanosheets on lotus thread devices for enhanced hydrophobicity and anti-microbial activity

Govarthini Seerangan Selvam[a], Thangaraju Dheivasigamani[a]*, Anusha Prabhu[b], Naresh Kumar Mani[b]*

[a]*Nano-crystal Design and Application Lab (n-DAL), Department of Physics, PSG Institute of Technology and Applied Research, Coimbatore-641062, Tamil Nadu, India.*

[b]*Microfluidics, Sensors and Diagnostics Laboratory (μSenD), Department of Biotechnology, Manipal Institute of Technology, Manipal Academy of Higher Education, Manipal 576104, Karnataka, India.*

Terms & Conditions

Author Information

Jump To

Corresponding Authors

Email: thangaraju@psgitech.ac.in

Naresh Kumar Mani - *Microfluidics, Sensors and Diagnostics Laboratory (µSenD), Department of Biotechnology, Manipal Institute of Technology, Manipal Academy of Higher Education, Manipal 576104, Karnataka India*; https://orcid.org/0000-0001-8245-3932;
Email: naresh.mani@manipal.edu

Authors

Govarthini Seerangan Selvam - *Nano-crystal Design and Application Lab (n-DAL), Department of Physics, PSG Institute of Technology and Applied Research, Coimbatore-641062, Tamil Nadu India*

Anusha Prabhu - *Microfluidics, Sensors and Diagnostics Laboratory (µSenD), Department of Biotechnology, Manipal Institute of Technology, Manipal Academy of Higher Education, Manipal 576104, Karnataka India*

Author Contributions

All authors contributed to the study conception and design. Material preparation, data collection and analysis were performed by S.S. Govarthini, D. Thangaraju, Anusha Prabhu and Naresh Kumar Mani. The first draft of the manuscript was written by S.S. Govarthini and D. Thangaraju, and all authors commented on previous versions of the manuscript. All authors read and approved the final manuscript. S.S. Govarthini: Writing - original draft. D. Thangaraju: Methodology, Conceptualization, Visualization, Methodology, Supervision, Writing - review and editing. Anusha Prabhu: Methodology, Writing - review and editing. Naresh Kumar Mani: Conceptualization, Visualization, Methodology, Supervision, Writing - review and editing.

Funding

D.T. sincerely thanks the Science and Engineering Research Board (ECR/2017/002974), Department of Science and Technology, Government of India, for the financial support. N.K.M. and A.P. acknowledge the financial support from Vision Group on Science and Technology, Government of Karnataka under SMYSR and RGS/F Scheme [Sanction Letter no.: KSTePS/VGST/SMYSR-2016-17/GRD-595/2017-18, KSTePS/VGSTRGS/F/GRD No.711/201711–18]. We extend our special thanks to the Department of Biotechnology, Manipal Institute of Technology.

Notes

The authors declare no competing financial interest.

References

Jump To

This article references 53 other publications.

1. Pandey, R.; Sinha, M. K.; Dubey, A. Cellulosic fibers from Lotus (Nelumbo nucifera) peduncle. *J. Nat. Fibers* **2020**, *17*, 298– 309, DOI: 10.1080/15440478.2018.1492486

| Google Scholar

3. Karthick, B.; Maheshwari, R. Lotus-inspired nanotechnology applications. *Resonance* **2008**, *13*, 1141– 5, DOI: 10.1007/s12045-008-0113-y

| Google Scholar

4. Bhushan, B.; Jung, Y. C.; Koch, K. Micro-, nano- And hierarchical structures for super-hydrophobicity, self-cleaning and low adhesion. *Philos. Trans R Soc. A Math Phys. Eng. Sci.* **2009**, *367*, 1631– 72, DOI: 10.1098/rsta.2009.0014

| Google Scholar

5. Holloway, P. J. Surface factors affecting the wetting of leaves. *Pestic. Sci.* **1970**, *1*, 156– 63, DOI: 10.1002/ps.2780010411

| Google Scholar

6. Ensikat, H. J.; Ditsche-Kuru, P.; Neinhuis, C.; Barthlott, W. Superhydrophobicity in perfection: The outstanding properties of the lotus leaf. *Beilstein J. Nanotechnol* **2011**, *2*, 152– 61, DOI: 10.3762/bjnano.2.19

| Google Scholar

7. Chang, C.; Chen, W.; Chen, Y.; Chen, Y.; Chen, Y.; Ding, F., et al. Recent Progress on Two-Dimensional Materials. *Acta Phys. - Chim Sin* **2021**, *37*, 2108017, DOI: 10.3866/PKU.WHXB202108017

| Google Scholar

8. Lv, R.; Robinson, J. A.; Schaak, R. E.; Sun, D.; Sun, Y.; Mallouk, T. E., et al. Transition Metal Dichalcogenides and Beyond: Synthesis, Properties, and Applications of Single- and Few-Layer Nanosheets. *Acc. Chem. Res.* **2015**, *48*, 56– 64, DOI: 10.1021/ar5002846

| Google Scholar

9. Zhou, X.; Sun, H.; Bai, X. Two-Dimensional Transition Metal Dichalcogenides: Synthesis, Biomedical Applications and Biosafety Evaluation. *Front Bioeng Biotechnol* **2020**, *8*, 236, DOI: 10.3389/fbioe.2020.00236

| Google Scholar

10. Vogel, E. M.; Robinson, J. A. Two-dimensional layered transition-metal dichalcogenides for versatile properties and applications. *MRS Bull.* **2015**, *40*, 558– 63, DOI: 10.1557/mrs.2015.120

| Google Scholar

11. Li, X.; Zhu, H. Two-dimensional MoS2: Properties, preparation, and applications. *J. Mater.* **2015**, *1*, 33– 44, DOI: 10.1016/j.jmat.2015.03.003

| Google Scholar

13. Eggertsen, F. T.; M. Roberts, R. M. Molybdenum Disulfide of High Surface Area. *J. Phys. Chem.* **1959**, *63*, 1981– 2, DOI: 10.1021/j150581a050

| Google Scholar

14. Gupta, D.; Chauhan, V.; Kumar, R. A comprehensive review on synthesis and applications of molybdenum disulfide (MoS2) material: Past and recent developments. *Inorg. Chem. Commun.* **2020**, *121*, 108200, DOI: 10.1016/j.inoche.2020.108200

| Google Scholar

15. Liu, T.; Liu, Z. 2D MoS2 Nanostructures for Biomedical Applications. *Adv. Healthc Mater.* **2018**, *7*, 1– 18, DOI: 10.1002/adhm.201701158

| Google Scholar

16. Zhu, C.; Zeng, Z.; Li, H.; Li, F.; Fan, C.; Zhang, H. Single-Layer MoS2-Based Nanoprobes for Homogeneous Detection of Biomolecules. *J. Am. Chem. Soc.* **2013**, *135*, 5998– 6001, DOI: 10.1021/ja4019572

| Google Scholar

17. Prabhu, A.; Singhal, H.; Giri Nandagopal, M. S.; Kulal, R.; Peralam Yegneswaran, P.; Mani, N. K. Knitting Thread Devices: Detecting Candida albicans Using Napkins and Tampons. *ACS Omega* **2021**, *6*, 12667– 75, DOI: 10.1021/acsomega.1c00806

| Google Scholar

18. Prabhu, A.; Giri Nandagopal, M. S.; Peralam Yegneswaran, P.; Singhal, H. R.; Mani, N. K. Inkjet printing of paraffin on paper allows low-cost point-of-care diagnostics for pathogenic fungi. *Cellulose* **2020**, *27*, 7691– 701, DOI: 10.1007/s10570-020-03314-3

| Google Scholar

19. Prabhu, A.; Nandagopal, M. S. G; Peralam Yegneswaran, P.; Prabhu, V.; Verma, U.; Mani, N. K. Thread integrated smart-phone imaging facilitates early turning point colorimetric assay for microbes. *RSC Adv.* **2020**, *10*, 26853– 61, DOI: 10.1039/D0RA05190J

| Google Scholar

20. Hasandka, A.; Singh, A. R.; Prabhu, A.; Singhal, H. R.; Nandagopal, M. S. G.; Mani, N. K. Paper and thread as media for the frugal detection of urinary tract infections (UTIs). *Anal Bioanal Chem.* **2022**, *414*, 847– 65, DOI: 10.1007/s00216-021-03671-3

| Google Scholar

22. Weng, X.; Kang, Y.; Guo, Q.; Peng, B.; Jiang, H. Recent advances in thread-based microfluidics for diagnostic applications. *Biosens Bioelectron* **2019**, *132*, 171– 85, DOI: 10.1016/j.bios.2019.03.009

| **Google Scholar**

23. Singhal, H. R.; Prabhu, A.; Giri Nandagopal, M. S.; Dheivasigamani, T.; Mani, N. K. One-dollar microfluidic paper-based analytical devices: Do-It-Yourself approaches. *Microchem J.* **2021**, *165*, 106126, DOI: 10.1016/j.microc.2021.106126

| **Google Scholar**

24. Hasandka, A.; Prabhu, A.; Prabhu, A.; Singhal, H. R.; Nandagopal, M. S. G; Shenoy, R., et al. Scratch it out": carbon copy based paper devices for microbial assays and liver disease diagnosis. *Anal Methods* **2021**, *13*, 3172– 80, DOI: 10.1039/D1AY00764E

| **Google Scholar**

25. Mani, N. K.; Das, S. S.; Dawn, S.; Chakraborty, S. Electro-kinetically driven route for highly sensitive blood pathology on a paper-based device. *Electrophoresis* **2020**, *41*, 615– 20, DOI: 10.1002/elps.201900356

| **Google Scholar**

26. Mani, N. K.; Prabhu, A.; Biswas, S. K.; Chakraborty, S. Fabricating Paper Based Devices Using Correction Pens. *Sci. Rep* **2019**, *9*, 1752, DOI: 10.1038/s41598-018-38308-6

| **Google Scholar**

27. Nilghaz, A.; Ballerini, D. R.; Shen, W. Exploration of microfluidic devices based on multi-filament threads and textiles: A review. *Biomicrofluidics* **2013**, *7*, 051501, DOI: 10.1063/1.4820413

| **Google Scholar**

28. Lin, S. C.; Hsu, M. Y.; Kuan, C. M.; Wang, H. K.; Chang, C. L.; Tseng, F. G. Cotton-based diagnostic devices. *Sci. Rep* **2014**, DOI: 10.1038/srep05769

| **Google Scholar**

29. Agustini, D.; Bergamini, M. F.; Marcolino-Junior, L. H. Characterization and optimization of low cost microfluidic thread based electroanalytical device for micro flow injection analysis. *Anal. Chim. Acta* **2017**, *951*, 108– 15, DOI: 10.1016/j.aca.2016.11.046

| **Google Scholar**

30. Agustini, D.; Bergamini, M. F.; Marcolino-Junior, L. H. Low cost microfluidic device based on cotton threads for electroanalytical application. *Lab Chip* **2016**, *16*, 345– 52,

31. Su, W. J.; Chang, H. C.; Shih, Y. T.; Wang, Y. P.; Hsu, H. P.; Huang, Y. S., et al. Two dimensional MoS_2/graphene p-n heterojunction diode: Fabrication and electronic characteristics. *J. Alloys Compd.* **2016**, *671*, 276– 82, DOI: 10.1016/j.jallcom.2016.02.053

| Google Scholar

32. Huang, Q.; Liu, M.; Chen, J.; Wan, Q.; Tian, J.; Huang, L., et al. Facile preparation of MoS_2 based polymer composites via mussel inspired chemistry and their high efficiency for removal of organic dyes. *Appl. Surf. Sci.* **2017**, *419*, 35– 44, DOI: 10.1016/j.apsusc.2017.05.006

| Google Scholar

33. Liu, Y.; Chen, Z.; Xie, W.; Song, S.; Zhang, Y.; Dong, L. In-situ growth and graphitization synthesis of porous Fe_3O_4/carbon fiber composites derived from biomass as lightweight microwave absorber. *ACS Sustainable Chem. Eng.* **2019**, *7*, 5318– 28, DOI: 10.1021/acssuschemeng.8b06339

| Google Scholar

34. Ko, T. J.; Hwang, J. H.; Davis, D.; Shawkat, M. S.; Han, S. S.; Rodriguez, K. L., et al. Superhydrophobic MoS_2-based multifunctional sponge for recovery and detection of spilled oil. *Curr. Appl. Phys.* **2020**, *20*, 344– 51, DOI: 10.1016/j.cap.2019.12.001

| Google Scholar

35. Zhu, T.; Shen, W.; Wang, X.; Song, Y. F.; Wang, W. Paramagnetic CoS_2@MoS_2 core-shell composites coated by reduced graphene oxide as broadband and tunable high-performance microwave absorbers. *Chem. Eng. J.* **2019**, *378*, 122159, DOI: 10.1016/j.cej.2019.122159

| Google Scholar

36. Chang, M.; Jia, Z.; He, S.; Zhou, J.; Zhang, S.; Tian, M., et al. Two-dimensional interface engineering of NiS/MoS_2/$Ti_3C_2T_x$ heterostructures for promoting electromagnetic wave absorption capability. *Compos Part B Eng.* **2021**, *225*, 109306, DOI: 10.1016/j.compositesb.2021.109306

| Google Scholar

37. Balouiri, M.; Sadiki, M.; Ibnsouda, S. K. Methods for in vitro evaluating anti-microbial activity: A review. *J. Pharm. Anal* **2016**, *6*, 71– 9, DOI: 10.1016/j.jpha.2015.11.005

| Google Scholar

38. Chou, S. S.; Kaehr, B.; Kim, J.; Foley, B. M.; De, M.; Hopkins, P. E., et al. Chemically exfoliated MoS_2 as near-infrared photothermal agents. *Angew. Chemie - Int. Ed* **2013**, *52*, 4160– 4, DOI: 10.1002/anie.201209229

| Google Scholar

| Google Scholar

40. French, A. D. Idealized powder diffraction patterns for cellulose polymorphs. *Cellulose* **2014**, *21*, 885– 96, DOI: 10.1007/s10570-013-0030-4

| Google Scholar

41. Schonfeld, B. B.; Huang, J. J.; Moss, S. C. The X-RAY system. *Z. Anorg. Allg. Chem.* **1965**, *338*, 404– 7

Google Scholar

42. Vasudevan, M.; Tai, M. J. Y.; Perumal, V.; Gopinath, S. C. B.; Murthe, S. S.; Ovinis, M., et al. Highly sensitive and selective acute myocardial infarction detection using aptamer-tethered MoS_2 nanoflower and screen-printed electrodes. *Biotechnol Appl. Biochem* **2021**, *68*, 1386– 95, DOI: 10.1002/bab.2060

| Google Scholar

43. Vasudevan, M.; Tai, M. J. Y.; Perumal, V.; Gopinath, S. C. B.; Murthe, S. S.; Ovinis, M., et al. Cellulose acetate-MoS_2 nanopetal hybrid: A highly sensitive and selective electrochemical aptasensor of Troponin I for the early diagnosis of acute myocardial infarction. *J. Taiwan Inst Chem. Eng.* **2021**, *118*, 245– 53, DOI: 10.1016/j.jtice.2021.01.016

| Google Scholar

44. Fang, L.; Catchmark, J. M. Structure characterization of native cellulose during dehydration and rehydration. *Cellulose* **2014**, *21*, 3951– 63, DOI: 10.1007/s10570-014-0435-8

| Google Scholar

45. Jorgensen, J. H.; Ferraro, M. J. Anti-microbial susceptibility testing: A review of general principles and contemporary practices. *Clin Infect Dis* **2009**, *49*, 1749– 55, DOI: 10.1086/647952

| Google Scholar

46. Loo, Y. Y.; Rukayadi, Y.; Nor-Khaizura, M. A. R.; Kuan, C. H.; Chieng, B. W.; Nishibuchi, M., et al. In Vitro anti-microbial activity of green synthesized silver nanoparticles against selected Gram-negative foodborne pathogens. *Front Microbiol* **2018**, *9*, 1555, DOI: 10.3389/fmicb.2018.01555

| Google Scholar

47. Sanguinetti, M.; Posteraro, B. Susceptibility testing of fungi to antifungal drugs. *J. Fungi* **2018**, *4*, 110, DOI: 10.3390/jof4030110

| Google Scholar

49. Basu, P.; Chakraborty, J.; Ganguli, N.; Mukherjee, K.; Acharya, K.; Satpati, B., et al. Defect-Engineered MoS_2 Nanostructures for Reactive Oxygen Species Generation in the Dark: Antipollutant and Antifungal Performances. *ACS Appl. Mater. Interfaces* **2019**, *11*, 48179– 91, DOI: 10.1021/acsami.9b12988

| Google Scholar

50. Alimohammadi, F.; Sharifian, M.; Attanayake, N. H.; Thenuwara, A. C.; Gogotsi, Y.; Anasori, B., et al. Antimicrobial properties of 2D MnO_2 and MoS_2 nanomaterials vertically aligned on graphene materials and Ti_3C_2 MXene. *Langmuir* **2018**, *34*, 7192– 200, DOI: 10.1021/acs.langmuir.8b00262

| Google Scholar

51. Pandit, S.; Karunakaran, S.; Boda, S. K.; Basu, B.; De, M. High antibacterial activity of functionalized chemically exfoliated MoS_2. *ACS Appl. Mater. Interfaces* **2016**, *8*, 31567– 73, DOI: 10.1021/acsami.6b10916

| Google Scholar

52. Zhao, Y.; Jia, Y.; Xu, J.; Han, L.; He, F.; Jiang, X. The antibacterial activities of MoS_2 nanosheets towards multi-drug resistant bacteria. *Chem. Commun.* **2021**, *57*, 2998– 3001, DOI: 10.1039/D1CC00327E

| Google Scholar

53. Liu, Y.; Wang, Y.; Yuan, X.; Prasad, G. The function of water absorption and purification of lotus fiber. *Mater. Sci. Forum* **2020**, *980*, 162– 7, DOI: 10.4028/www.scientific.net/MSF.980.162

| Google Scholar

Cited By

Jump To

This article has not yet been cited by other publications.